Geo-Marine Letters (1999) 19: 97–110

P. R. Vogt · J. Gardner · K. Crane · E. Sundvor
F. Bowles · G. Cherkashev

Ground-truthing 11- to 12-kHz side-scan sonar imagery in the Norwegian–Greenland Sea: Part I: Pockmarks on the Vestnesa Ridge and Storegga slide margin

Abstract Numerous small (50- to 300-m-diameter) strong-backscatter objects were imaged on the 1200- to 1350-m deep crest of Vestnesa Ridge (Fram Strait) and along the 900- to 1000-m deep northeast margin of the Storegga slide valley. Ground-truthing identified most of these objects as 2- to 10-m-deep pockmarks, developed within soft, acoustically stratified silty clays (typical wet bulk density: 1400–1600 $kg\,m^{-3}$; sound speed: 1480–1505 $m\,s^{-1}$; porosity, 65–75%; shear strength: 5–10 kPa; water content: 80–120%; and thermal conductivity: 0.8–0.9 $W\,m^{-1}\,deg\,C^{-1}$ in the top 3 m). Gas wipeouts, enhanced reflectors, and reflector discontinuities indicate recent or ongoing activity, but the absence of local heat flow anomalies suggests that any upward fluid flows are modest and/or local.

Introduction: SeaMARC II side-scan spots

Little was known in plan view about sea-floor features in the Norwegian–Greenland Sea at spatial scales that are less than a few kilometers until detailed SeaMARC II side-scan sonar and swath bathymetric mapping (Shor 1990) began there in 1989–1990 (Vogt et al. 1991; Crane et al. 1995). Although numerous profiles had been collected, generally at random spacings and orientations, it was commonly impossible to identify the features from their cross-sections, and many objects were missed entirely. For example, isometric features such as pockmarks and diapirs (Fig. 1) were difficult to distinguish from linear features such as channels or sediment waves. The new side-scan imagery revealed a wealth of features, many of uncertain origin and/or state of activity. In this paper we discuss just one type of feature (Vogt et al. 1994), appearing in the SeaMARC II side-scan imagery as clusters of small spots, each of the order of 50–300 m in diameter, and in all cases exhibiting elevated acoustic backscatter relative to the surrounding sea floor. (The SeaMARC II system was uncalibrated, so absolute scattering strength could not be recovered.)

The small size of these spots places them near the limit of resolution for 11- to 12-kHz systems. They are generally too small to be resolved with the lower-frequency (6.5-kHz) GLORIA system, which has also been extensively deployed in the Norwegian–Greenland Sea (e.g., Dowdeswell et al. 1996), although not precisely in the areas described in this paper. (GLORIA can, however, resolve extensive "hard grounds" that may exist with the pockmarks). The strong-backscatter spots we mapped were not accompanied by a measurable bathymetric anomaly in the swath bathymetry; indeed, the spots are so small that we did not expect to resolve them in the swath contours. We were uncertain of the type of object until correlation with an archived 3.5-kHz profile through one of the "spotted" areas (Vogt et al. 1994). Although navigation uncertainties did not permit a one-to-one correlation of features between the 3.5-kHz data and the side-scan image, the profile did assure us that we were dealing with small sea-floor craters (depressions) now widely referred to as pockmarks (Hovland and Judd 1988).

The small strong-backscatter spots were imaged using *F/S Håkon Mosby* in 1989–1990 on the crest of Vestnesa Ridge in Fram Strait (Figs. 1 and 2) (Vogt et al. 1994) and

P. R. Vogt (✉) · J. Gardner
Code 7420, Naval Research Laboratory, 4555 Overlook Ave. SW, Washington, DC 20375-5320, USA

K. Crane
Hunter College, CUNY, New York, USA

E. Sundvor
Institute of Solid Earth Physics, University of Bergen, Bergen, Norway

F. Bowles
Code 7431, Naval Research Laboratory, Stennis Space Center, MS 39529-5004, USA

G. Cherkashev
VNIIOkeangeologiya, St. Petersburg, Russia

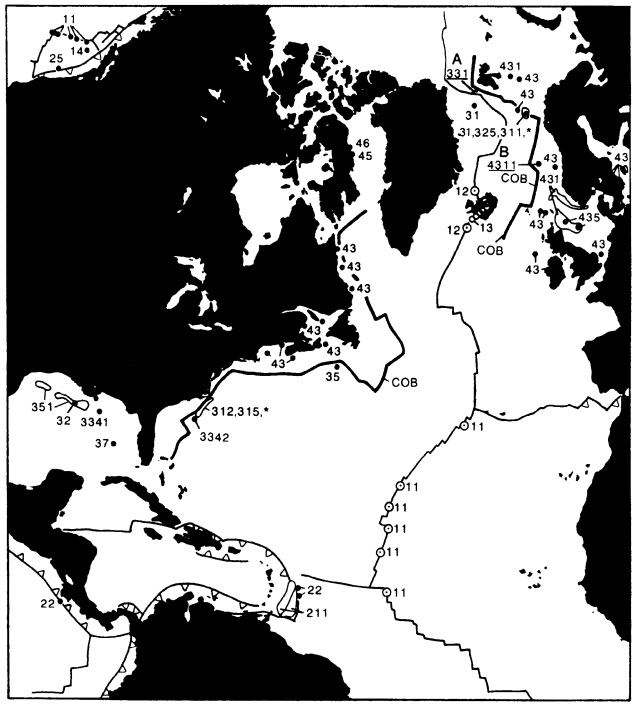

Fig. 1 Active or recently active sea-floor gas and/or water venting sites (or areas) and associated diapir fields in the North Atlantic region. Compiled from numerous sources, particularly Hovland and Judd (1988). Pockmark areas discussed in this paper are (A) Vestnesa Ridge and (B) Storegga Margin. The first digit in a label denotes tectonic setting and the following digits denote classes or combinations of vent features or abundance: (1) Mid-Oceanic Ridge (MOR): 11, hot, deep vents; 12, hot, shallow vents (<500 m); 13, Iceland hydrothermal areas; 14, off-axis MOR lower temperature vents. (2) Subduction zone: 21 diapirs (211, numerous; 212, scattered); 22, mud volcanoes; 25, gas seeps. (3) Older oceanic crust and continent–ocean crustal boundary (COB): 31, diapirs (312, scattered; 315, diapirs with gas seeps); 32, mud volcano (325, mud volcano and gas seep); 33, gas eruption feature (3341, eruption crater; 3342, eruption collapse feature; 331, pockmark field); 35, gas seep (351, numerous); 37, hypersaline seep. (4) Continental shelf: 43, gas eruption feature (43, isolated pockmarks; 431, pockmark field; 4311, pockmarks and mounds; 435, pockmark with gas seep); 46, fresh-water spring. * Major slump or slide spatially associated with vent phenomena

in the Storegga slide area on *R/V Maurice Ewing* in 1990. The latter location is ca. 15–20 km north of the north wall of the slide valley. Judged from the shape and size of the strong-backscatter spots, the Storegga-margin pockmarks are on average somewhat larger and more circular than their Vestnesa counterparts. The spots are typically spaced 0.5–3 km from their nearest neighbors. In both areas the background backscatter is relatively weak and essentially featureless; the fine-scale speckle in the data (Figs. 3A, 4A, and 7A) is attributed to various noise sources and is not reproducible from one ensonification experiment to another. It is not obvious why pockmarks should invariably appear as strong-backscatter spots in the side-scan imagery. This puzzle is discussed at the very end of the paper.

Unlike most previously known pockmarks (Fig. 1; see also Hovland and Judd 1988), the ones studied here are located beyond the continental shelf edge at water depths of 900–1000 m (Storegga margin) and 1200–1350 m (Vestnesa Ridge). Vogt et al. (1994) suggested that the Vestnesa pockmarks were caused by episodic methane release from gas trapped below a natural anticline structure formed by a gas hydrate carapace. Seismic data suggest gas hydrates are present in the region of both pockmark areas (Eiken and Hinz 1993; Mienert and Bryn 1997).

In 1995 and 1996 we revisited the two putative pockmark areas to ground-truth the acoustic imagery. The following questions were addressed: (1) Are the strong-backscatter spots actually pockmarks, and if so, what is their morphology and subbottom structure? (2) What are the characteristics that could explain the relatively strong backscatter of the features? (3) Are the area sediments soft and fine, as suggested to be favorable for pockmark formation (Hovland and Judd 1988)? (4) Are there other relevant sea-floor features, not detected by the 11- to 12-kHz imagery? (5) What is the origin of these pockmarks? (6) Are there local heatflow anomalies associated with the pockmarks or with the local areas in which they occur, given that upward flow of fluid can steepen subbottom thermal gradients (Wright and Louden 1989)? This last point may help to explain the heatflow highs known from the Norwegian-Barents-Svalbard continental margin (Vogt and Sundvor 1996).

Ground-truth data

As part of the SeaMARC II ground-truth cruises in 1995 (*F/S Håkon Mosby*) and 1996 (*NIS Professor Logachev*), both areas were investigated where the 11- to 12-kHz imagery had imaged supposed pockmarks. the Håkon Mosby conducted two close-spaced 3.5-kHz and 38-kHz surveys of the principal pockmark areas on the Vestnesa Ridge (Figs. 2, 3B, 4B, and 5). The track separation was ca. 900 m. Upon conclusion of these site surveys, several gravity cores, one box core, and several heatflow stations were located in the most promising sites (Table 1). Attempts were made to measure heat flow and collect cores both from within pockmarks and just outside them. However, station-keeping in water depths more than 10 times the object diameter was inadequate to guarantee that the interiors of pockmarks had been sampled.

In 1996 a similar strategy was employed to ground-truth an area of supposed pockmarks discovered in SeaMARC II data in the Storegga slide area. The pockmarks represent a WNW extension of an area of "fluid-escape structures" descibed by Evans et al. (1996). The Logachev conducted a detailed site survey of the pockmark area with its 8-kHz profiler, which was used both for bathymetry and shallow subbottom profiling (Figs. 6, 7B, and 8). The track spacing was 500 m. Again, we attempted to collect gravity cores and measure heat flow both inside

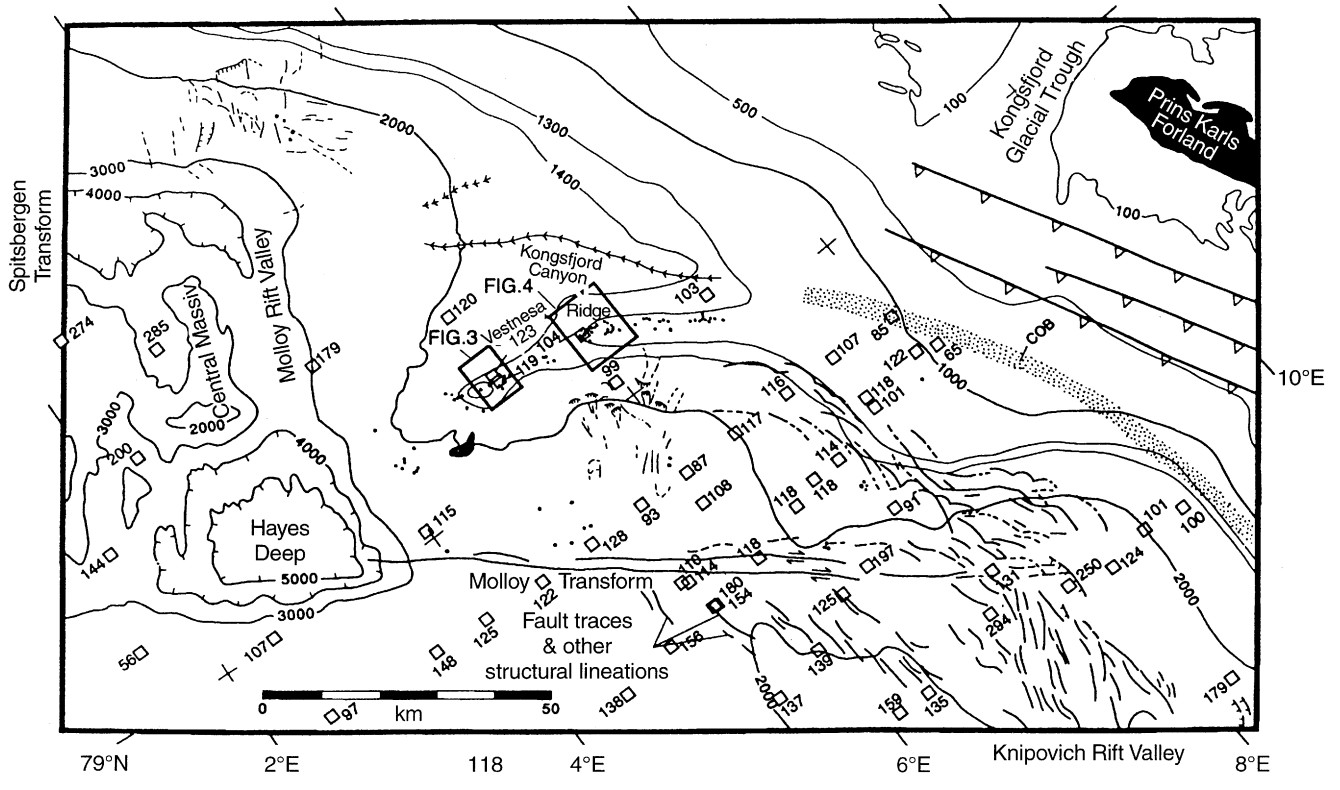

Fig. 2 Vestnesa ridge area (adapted from Vogt et al. 1994) showing pockmarks (dots), structural lineations (SL, thick, solid or dashed lines) interpreted from side-scan, debris flow scars (thin lines), bathymetric contours (m), submarine channels (notched lines), and outcrops (black). COB: continent–ocean crustal boundary. Heat-flow stations are in mW m^{-2}. Boxes show locations of Figs. 3 and 4

and outside a prominent pockmark (Table 1). Physical properties were measured on the cores, which were raised in hard PVC liners, cut into 1-m lengths, and sealed for measurements to be made in advance of opening. The 1995 cores from Vestnesa Ridge were measured for thermal conductivity on board ship, and the 1996 cores at the University of Bergen. The measurements were made at 10-cm intervals by drilling small holes through the PVC liner and inserting a Fenwal probe. This needle probe consists of a thermistor and a heating wire, with the thermistor resistance measured every 5 s for 2 min. The small holes were then sealed with glue to avoid sediment desiccation. The thermal conductivity data (corrected for in-situ conditions) for the pockmark area cores is shown in Fig. 9.

In addition, the 1995 *Mosby* cores were continuously logged at Texas A&M University for gamma-ray attenuation and compressional (sound) wave speed, using the Tamu Geotek Logger (Sawyer et al. 1997). Measurements were made at 2-cm intervals along the cores except near the ends of the 1-m sections, where disturbance was expected. Wet bulk density, porosity, water content, and void ratio were calculated from the attenuation data. Some of these parameters, along with sound speed, are plotted against subbottom depth in Fig. 10. In addition, measurements of density, shear strength, and grain size were made after the cores were opened in 1998 (Fig. 10).

Five successful heatflow values were obtained from the three pockmark areas (Table 1): stations were located in the eastern Vestnesa survey area (one), in the western Vestnesa area (two), and in the Storegga pockmark province (two). The same "Lamont heat-flow probe" (Crane et al. 1988) was used to measure the thermal gradient, from which the actual conductive heat flow was computed from the core-averaged thermal conductivity from nearby sediment cores (Table 1, Fig. 9). The probe comprises four or five thermistors mounted on outriggers several centimeters away from a solid lance that is attached to a core head weight. The instrument is dropped into the bottom and left several minutes, enabling correction for frictional heating. The probe monitors bottom water temperature and instrument tilt. Full penetration (4.7 m) was achieved at each of the pockmark sites due to the soft character of the sediment. Temperatures increased linearly with depth, with little scatter. This suggests bottom-water temperature changes over the previous months to a few years were minimal. Vogt and Sundvor (1996) discussed such effects.

Bathymetry

Bathymetric data maps were hand-contoured from plots of digitally recorded soundings for the pockmark areas

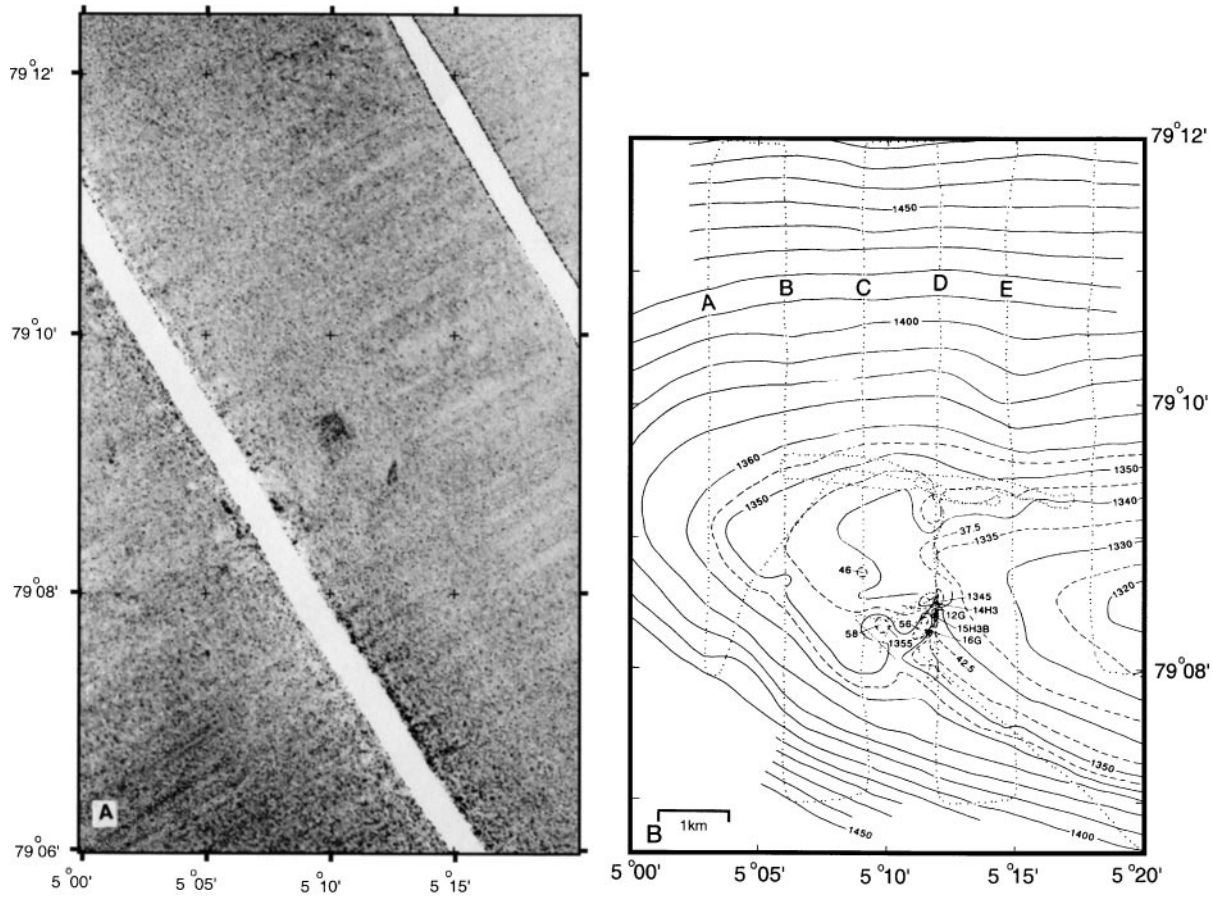

Fig. 3 (A) SeaMARC II side-scan sonar image of western part of Vestnesa ridge crest. Darker tones denote stronger backscatter. Small dark patches interpreted as pockmarks. See Fig. 2 for location. (B) Bathymetric contours (m) based on 38-kHz soundings (dots) corresponding to A. The first two digits have been dropped from some soundings to reduce clutter. Håkon Mosby station numbers are followed by HF (heatflow), G (gravity core) or B (box core)

(Figs. 3B, 4B, and 7B). Due to the accurate GPS-based navigation and the relatively smooth bottom topography, water depth discrepancies at track crossings were generally only about 2 m. The Vestnesa contours are drawn at 10-m intervals, locally reduced to 5 and even 2.5 m on the ridge crest where the pockmarks are located. Only at such small contour intervals, and with the addition of spot soundings to the nearest meter, are pockmarks visible in the bathymetry (Figs. 3B and 4B). In the Storegga margin pockmark area, depth contours are drawn at 5-m intervals (Fig. 7B), and track intersection discrepancies are in the range of a few meters. However, there is more ping-to-ping noise in the digital soundings here, perhaps because of the lower frequency used (8 kHz vs. 38 kHz on Vestnesa Ridge). In general, pockmark-scale features a few meters deep could not be reliably contoured in the Logachev bathymetry.

The bathymetric chartlets produced from contouring single-beam data (Figs. 3B, 4B, and 7B) are higher in resolution and accuracy than the SeaMARC II-based swath bathymetry available from the 1989–1990 side-scan cruises. We, therefore, do not show the latter in this paper (see Crane et al. 1995). However, analysis of the SeaMARC II center beam returns (i.e., treating the nadir returns as echosoundings) shows that pockmarks of ca. 2–3 m depth and 200 m diameter were recorded on some crossings of Vestnesa Ridge (C. Nishimura personal communication 1998). Obviously these nadir features were not recorded in the side-scan data as backscatter objects on the same traverse.

Comparison of the bathymetric contours and profiles with the side-scan imagery produced mixed results. On Vestnesa Ridge, correlation between the pockmarks shown in the contours (Figs. 3B and 4B) and the side-scan objects was unsatisfactory. We attribute this to navigation and pixel placement errors of the 1989 SeaMARC II data and to the probable existence of pockmarks between the profiles. At a spacing of 900 m, the profiles were likely to miss many of the side-scan spots 50–300 m across. Less likely, but possible, is the existence of side-scan spots, caused entirely by subbottom features, for example gas bubbles a few meters below the bottom, with no recognizable expression in the 3.5-kHz profiles. We can say with certainty only that the area of the bathymetrically mapped

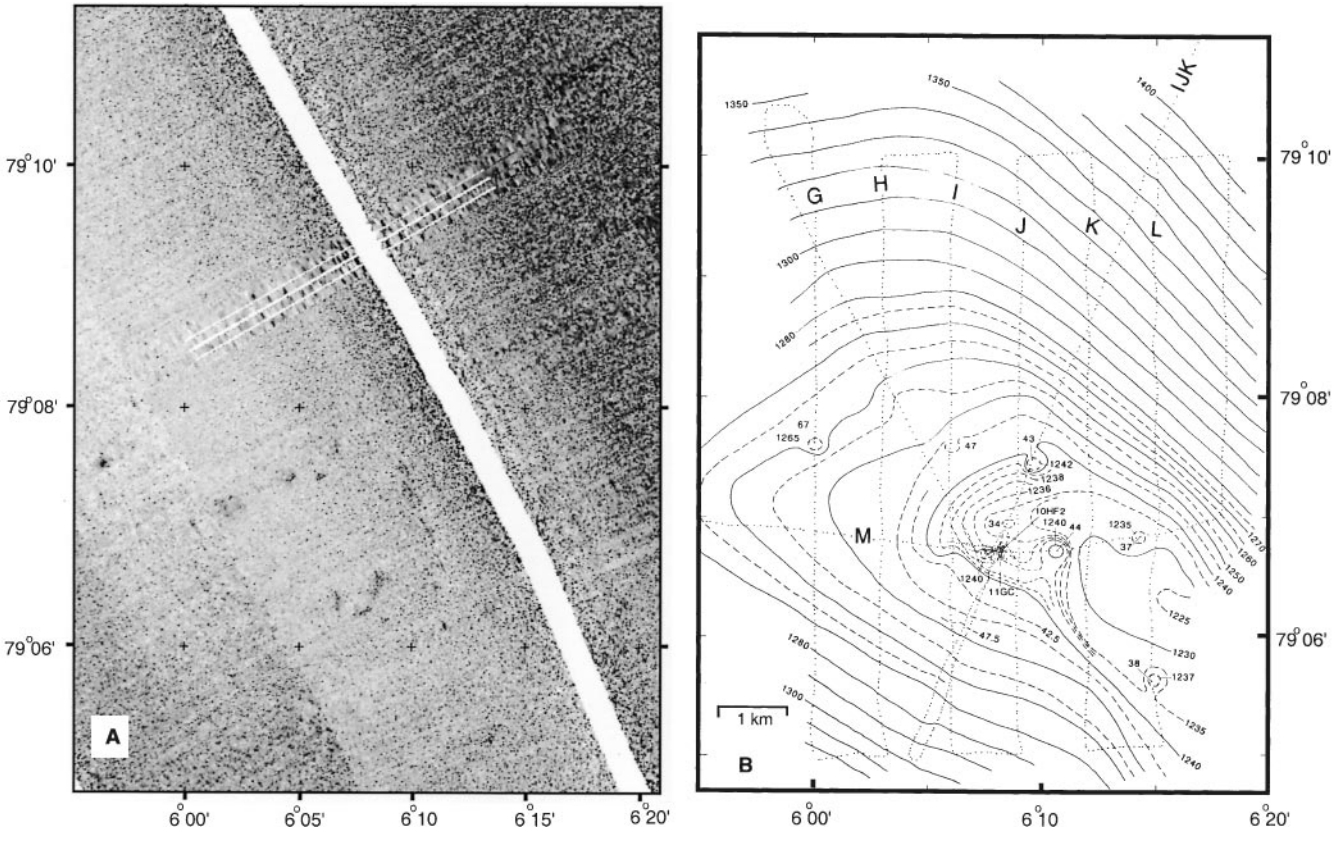

Fig. 4 (A) SeaMARC II side-scan sonar image of eastern Vestnesa ridge crest. (B) Corresponding bathymetry and station locations. See Fig. 3 for captions

pockmarks (Figs. 3B and 4B) corresponds to the area within which the backscatter objects occur (Figs. 3A and 4A).

The *Logachev* survey of the Storegga pockmark data showed poor correlation between digitally recorded bathymetry and the backscatter spots mapped with SeaMARC II. However, the locations of pockmarks seen in the 8-kHz profiles (Fig. 8) show excellent agreement in size and location with the location of the spots in almost all cases (Fig. 7B). All major spots were verified as pockmarks, and all pockmarks on the profiles were picked up on the side-scan imagery.

However, several small mounds crossed by the 8-kHz profiler (Figs. 7B and 8) were not detected in the side-scan imagery (Fig. 8A). There are several possible reasons: (1) the mounds are smaller than the pockmarks in terms of diameter and relief (ca. 2 m) and thus create a smaller topographic backscatter effect (discussed below); (2) the mounds seen in the 8-kHz profiles occur in the outer, lower-grazing angle part of the SeaMARC II swath, where resolution is expected to be worse; and (3) if the mounds are embryonic pockmarks (following Hovland and Judd 1988), the methane that will eventually erupt to form the pockmark may still be trapped at depth. Thus, a variety of methane-escape features that could enhance the backscatter strength of pockmarks (numerous unit pockmarks, residual coarse sediment, authigenic carbonate, gas bubbles, and hard benthic organisms such as clams) may not occur on the mounds.

A main conclusion from the detailed bathymetric maps is that the Vestnesa Ridge pockmarks are largely or entirely confined to a ca. 3-km-wide belt centered on the ridge crest, as concluded on the basis of less accurate bathymetric data by Vogt et al. (1994). Apparently conditions for pockmark development are not suitable on ridge slopes greater than ca. 20 : 1000. The Vestnesa pockmarks in the two survey areas occur in water depths of 1330–1360 m in the western area and 1230–1270 m in the eastern area.

In comparison, the approximately half-dozen Storegga margin pockmarks examined (Figs. 7 and 8) occur between 960 and 1020 m water depths, on a WNW-dipping sea floor with a slope of 6:- to 8 : 1000, consistent with the same slope dependence suggested for the Vestnesa pockmarks. A gentle westward-convex contour shape in the central part of the survey area (Fig. 7B) suggests the existence of a slight swell with ca. 5-m relief, that may be associated with the pockmarks, all of which can be enclosed by an elliptical area ca. 3 km in width. The gentle swell may be the surface topographic expression of a buried sidewall scarp, marking an older, perhaps preglacial slide (Evans et al. 1996). Additional pockmarks and other fluid escape structures are known to exist to the

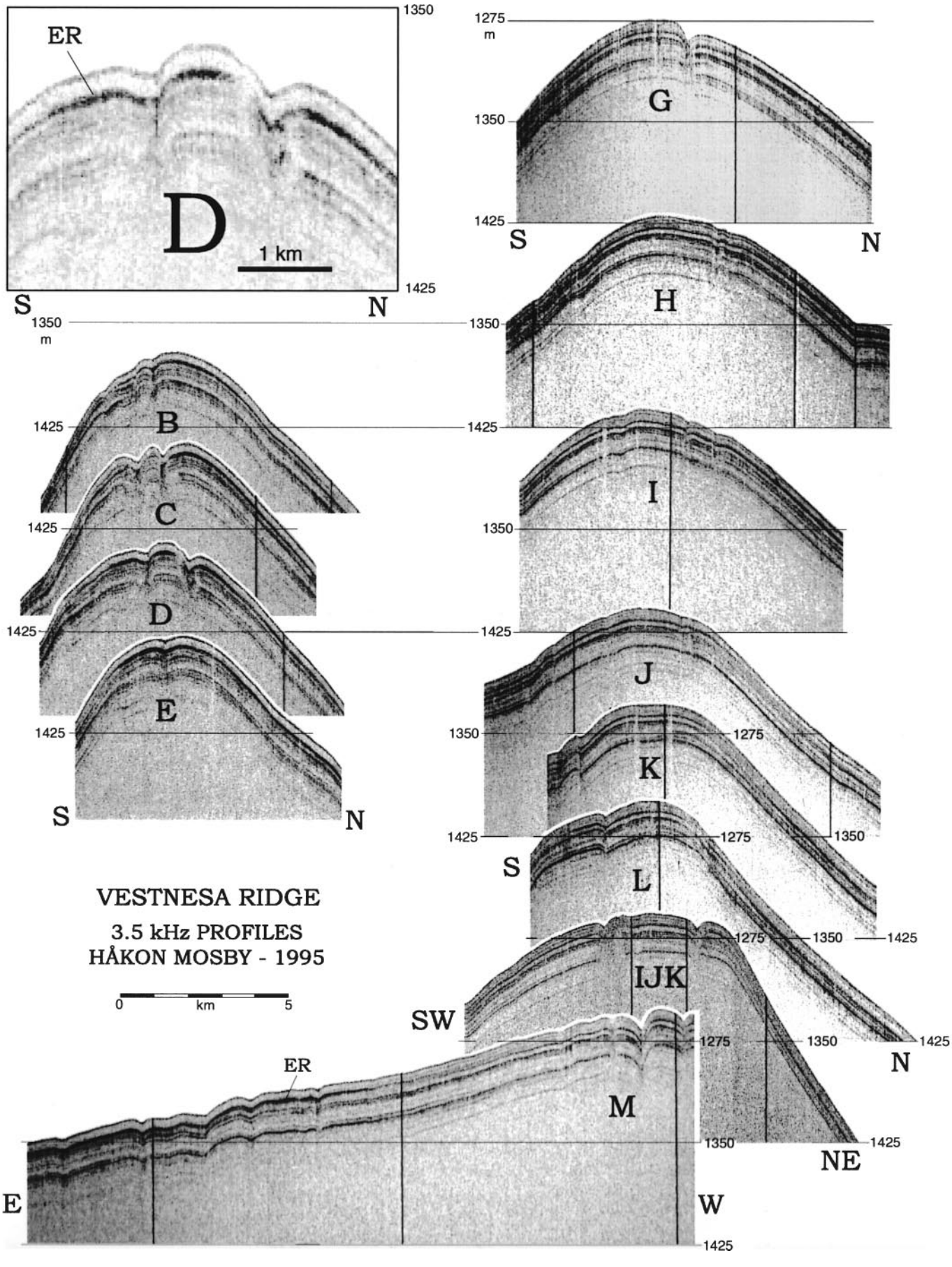
ER
D
1 km
1350
1425
S
N
1275
m
G
1350
1425
S
N
H
1350
1425
B
1425
C
1425
D
1425
E
1425
S
N
I
1350
1425
J
1350
1275
K
1425
1275
1350
S
L
1275
1350
1425
IJK
SW
1275
1350
1425
N
ER
M
1350
1425
NE
E
W
1425
VESTNESA RIDGE
3.5 kHz PROFILES
HÅKON MOSBY - 1995
0
km
5

Table 1 Pockmark area heatflow and conductivity[a]

Area	Lat.	Long.	D (m)	Station	Therm.	Pen. (m)	mK m^{-1}	W m^{-1}K^{-1}	mW m^{-2}
Vestnesa (E)	79°06.9′N	6°00.2′E	1238	HM-16B-10 (HF10)	4	4.70	116 ± 8	0.9	104
Vestnesa (W)	79°08.4′N	5°11.8′E	1342	HM-16B-14 (HF3A)	4	4.70	145 ± 9	0.85	123
Vestnesa (W)	79°08.5′N	5°12.0′E	1342	HM-16B-15 (HF3B)	4	4.70	140 ± 10	0.85	119
Storegga	64°49.4′N	4°18.3′E	967	PL-096-6 (HF2A)	5	4.70	59.7 ± 1.9	0.86	51
Storegga	64°49.14′N	4°18.5′E	969	PL-096-6 (HF2B)	5	4.70	56.2 ± 1.8	0.86	48
Vestnesa (E)	79°06.7′N	6°08.2′E	1237	HM-16B-11	N.A.	2.80	N.A.	0.9	N.A.
Vestnesa (W)	79°08.5′N	5°11.9′E	1349	HM-16B-12	N.A.	3.00	N.A.	0.85	N.A.
Vestnesa (W)	79°08.3′N	5°11.7′E	1346	HM-16B-16	N.A.	3.00	N.A.	0.85	N.A.
Storegga	64°49.13′N	4°18.5′E	968	PL-096-8 (P-1-3)	N.A.	3.33	N.A.	0.86	N.A.
Storegga	64°49.45′N	4°18.6′E	967	PL-096-9 (P-1-4)	N.A.	3.35	N.A.	0.86	N.A.

[a] Heatflow and thermal conductivity stations on 1995 *Håkon Mosby* (HM) and 1996 *Professor Logachev* (PL) cruises. D is water depth, Therm. is number of thermistors on probe, and Pen. denotes subbottom penetration in meters.

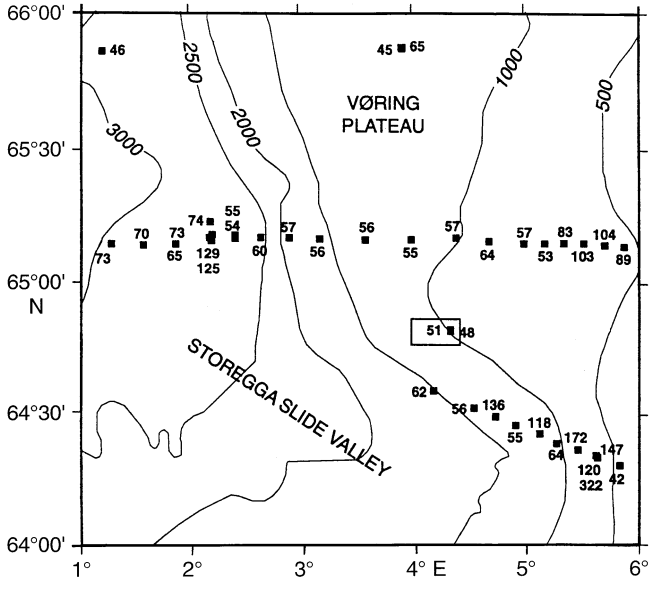

Fig. 6 Storegga slide, northern margin bathymetry (contours in meters), heatflow stations (mW m^{-2}, from Sundvor et al. 1999), and location of SeaMARC II-imaged pockmarks and ground-truthing survey (box)

northeast of our area, along or just north of the ESE continuation of the buried escarpment.

Echo character and subbottom structure

Subbottom structure was mapped at 3.5 kHz on Vestnesa Ridge (Fig. 5) and 8 kHz in the Storegga area (Fig. 8).

Fig. 5 3.5-kHz profiles across Vestnesa Ridge. See Fig. 2A and B for locations. "ER" denotes example of enhanced reflector. Note portion of profile D enlarged at upper left

Maximum penetration away from pockmarks or mounds was about 25–50 m on Vestnesa Ridge and 20–30 m in the Storegga area. The penetration difference between the areas probably reflects the difference in frequency, with less penetration at 8 than at 3.5 kHz. Away from the pockmarks and mounds, the echo character is of type IB (Damuth 1978; Pfirman and Kassens 1995), i.e. "sharp continuous echoes with numerous parallel subbottoms." Numerous cores raised from this type of sea floor show fine-grained hemipelagic-type sediments with an average of only 1% bedded coarser sediment (sand and silt). Our profiles reveal no evidence of faulting or mass wasting down to the acoustic penetration limit.

The profiles show many of the Vestnesa pockmarks and at least one of the Storegga pockmarks (no. 2, Fig. 8) with subbottom reflectors simply down-bowed under the pockmarks, with no disruption or acoustic wipeouts often seen under pockmarks (Hovland and Judd 1988). Narrow disturbances may have been missed, if profiles did not cross the pockmark centers. However, it appears that a number of pockmarks, mostly on Vestnesa Ridge, simply exhibit down-bowed continuous reflectors. We offer two scenarios to explain this: (1) The pockmarks may have formed in the past and are not currently active. Hemipelagic sediments deposited subsequent to activity would appear conformably draped, as observed. (2) The pockmarks may have formed by withdrawal of gas or fluid at depth – for example, by hydrate dissociation – causing a small area of seafloor to collapse. This type of pockmark formation, if real, would be one not previously recognized (e.g., Hovland and Judd 1988).

A profile collected at 15 km h^{-1} crosses a 200-m pockmark in less than 1 min. This circumstance, coupled with the wide beam of the outgoing acoustic pulse, limits the resolution of subbottom structure in our profiles (Figs. 5 and 8). One cannot always be sure whether the subbottom reflectors continue under the pockmark or are disrupted by gas or pore fluid rise. Running the profiler while the vessel attempts to keep station above the feature may provide the necessary data. For example, keeping station above feature 9 (right side of the long profile in Fig. 8)

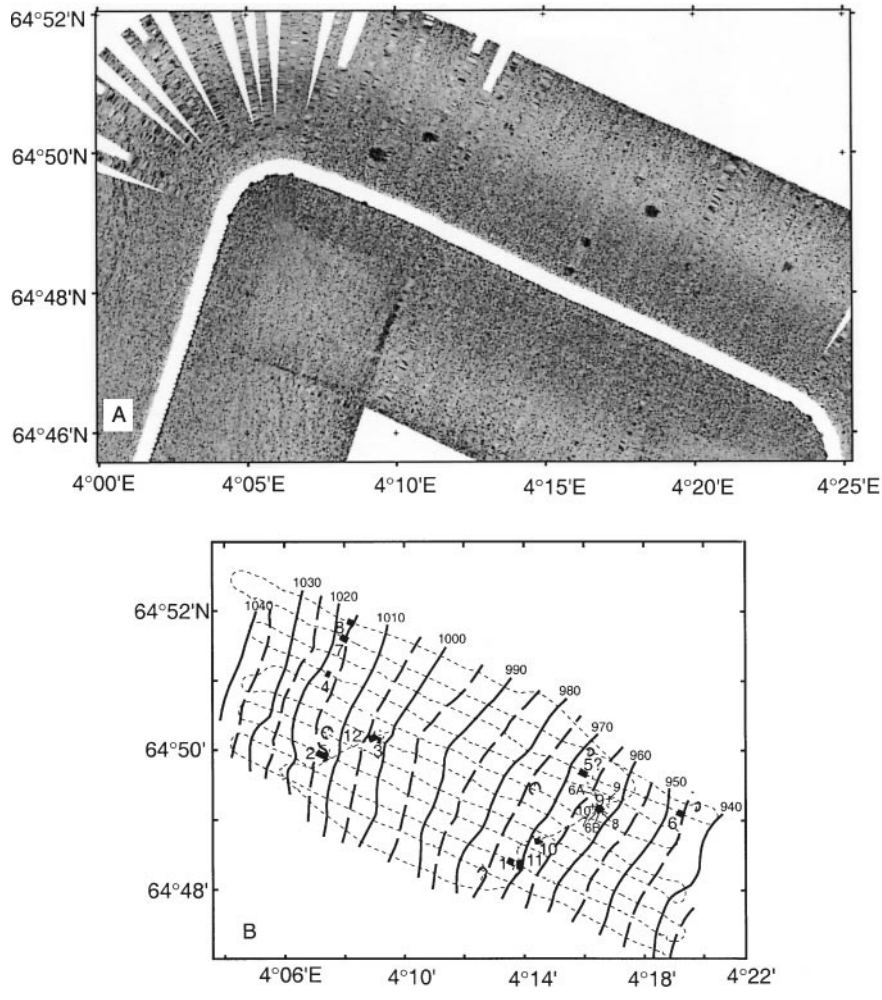

Fig. 7 **A** SeaMARC II sidescan sonar image of pockmarks (darker spots) on Storegga slide margin (see Fig. 6 for location). Darker tones correspond to stronger backscatter. **B** Bathymetric contours for northern portion of (A), in meters, with dots showing locations of soundings. Pockmarks and mounds are numbered (see Fig. 8). Heatflow stations and gravity cores are labeled with small-sized numerals, corresponding to "PL" station in Table 1

clearly shows that reflectors do not continue across the pockmark, which thus appears to be presently active. (The complex curved returns from "within" the pockmark are interpreted as bathymetric reflections from the inner wall of the pockmark crater).

In the Storegga area, we discovered small mounds in the 8-kHz profiler data (Fig. 8, features 4, 6, 7, 8; see Fig. 7B). No such mounds were discovered in the Vestnesa profiles. The Storegga mounds do not appear in the SeaMARC II side-scan data (Fig. 7A), perhaps because of their low relief (a few meters) or because of their location in the higher-noise, outer part of the SeaMARC II swath. Hovland and Judd (1988) postulate that mounds of this type represent embryonic pockmarks, with gas having collected at depth and, some time in the future, venting forcefully to form new pockmarks.

Except for the profile across pockmark 2 (Fig. 8), both mounds and pockmarks in the Storegga area are underlain by columnar disturbances (acoustic voids) extending from the sea floor down to the deepest recorded reflector levels. In some examples (nos. 1, 9, 10 of Fig. 8) the acoustic void appears to extend laterally beyond the pockmark lips. Subbottom reflectors generally disappear within the acoustic voids, but locally continue with reduced reflector strength (nos. 3, 4, 9 of Fig. 8). Reflectors appear bowed upward (or downward) as mounds (or pockmarks) are approached from the outside (nos. 7, 8, or 9). Some pockmarks exhibit raised rims (nos. 1, 3, 11, 12 of Fig. 8), perhaps reflecting remnants of prepockmark mounds or debris erupted from the pockmarks. In those cases subbottom reflectors are also bowed upwards under the pockmark rims. In other cases the subbottom reflectors continue unbowed up to edge of the acoustic void (nos. 1, 4, 10 of Fig. 8).

Following Hovland and Judd (1988), we attribute the acoustic voids and reflector deformation to methane gas or slightly pressurized porewater, which has risen through the sediment and disrupted the original acoustic stratification. There are only minor examples of possible acoustic turbidity, for example, under the northern pockmarks on profiles C and D (Fig. 5), and even these may be

Fig. 8 Portions of 8-kHz profiler records, showing pockmarks and mounds. See Fig. 7B for feature locations

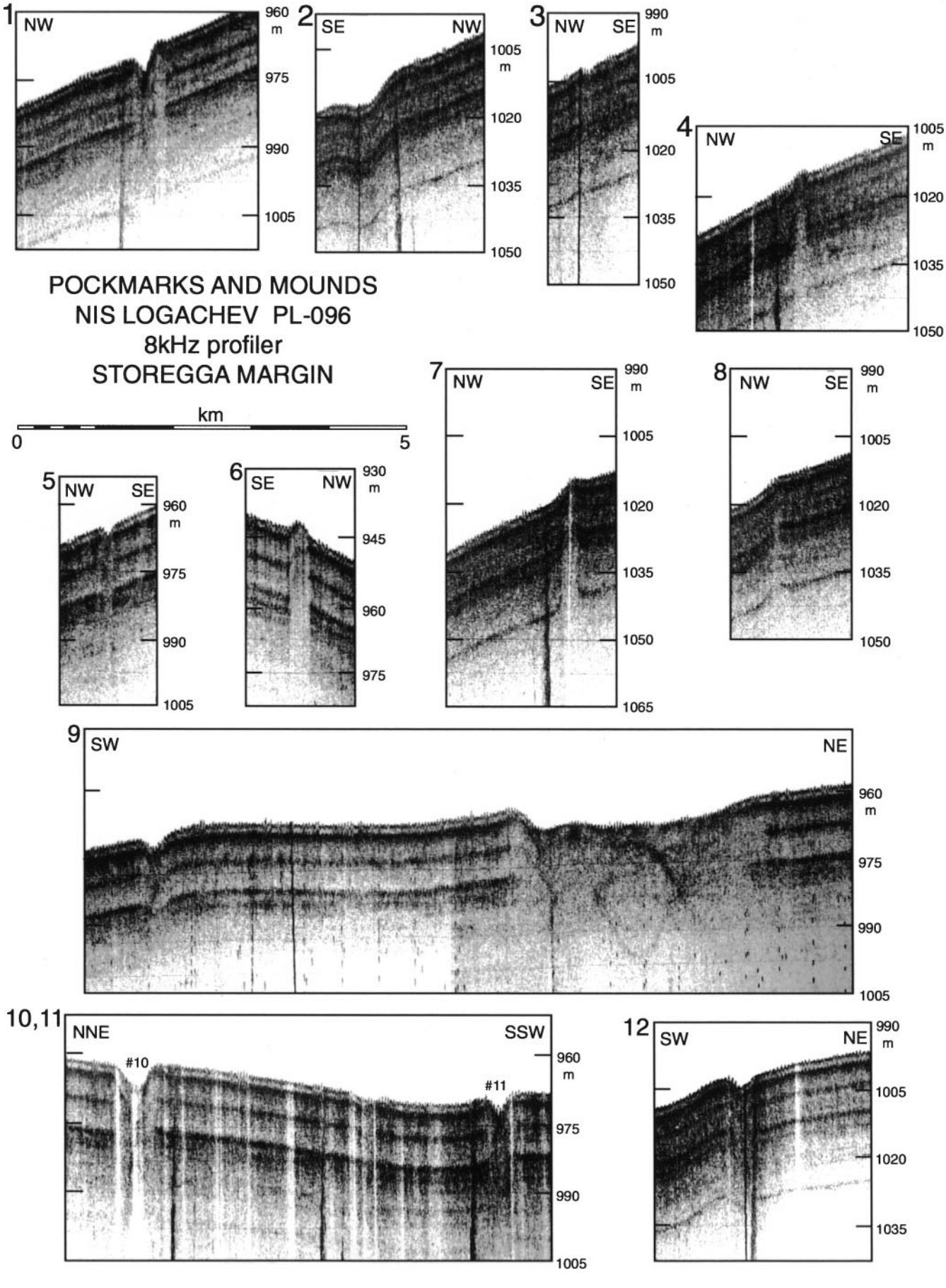
1
NW
960 m
975
990
1005
2
SE
NW
1005 m
1020
1035
1050
3
NW
SE
990 m
1005
1020
1035
1050
4
NW
SE
1005 m
1020
1035
1050
POCKMARKS AND MOUNDS
NIS LOGACHEV PL-096
8kHz profiler
STOREGGA MARGIN
km
0
5
5
NW
SE
960 m
975
990
1005
6
SE
NW
930 m
945
960
975
7
NW
SE
990 m
1005
1020
1035
1050
1065
8
NW
SE
990 m
1005
1020
1035
1050
9
SW
NE
960 m
975
990
1005
10,11
NNE
SSW
#10
#11
960 m
975
990
1005
12
SW
NE
990 m
1005
1020
1035

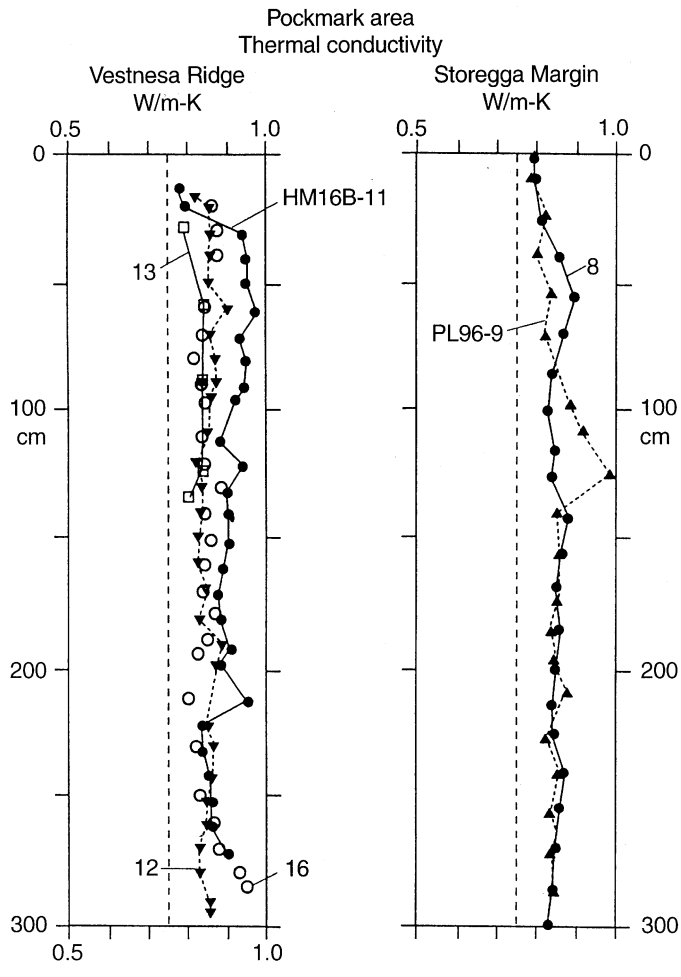

Fig. 9 Thermal conductivity vs. subbottom depth, measured on gravity cores (see Figs. 3B, 4B, and 7B and Table 1 for locations). "HM," *F/S Håkon Mosby* 1995 cores; "PL", *NIS Professor Logachev* cores

subbottom acoustic focusing effects rather than actual acoustic turbidity. Some coherent reflectors appear locally enhanced, for example, locally under the ridge crest on profiles C, D, and E, and under the western portion of M (Fig. 5). Such reflector enhancement may be due to gas bubbles trapped at certain stratigraphic levels, but if so the amount of free gas must be very small, otherwise underlying reflectors would not be seen. Furthermore the enhanced reflectors are not closely associated with pockmarks. We therefore judge the present free gas concentration to be relatively slight, at least in the upper 20–50 m visible to our profiler, below the Vestnesa Ridge.

Conductivity and heat flow

There is no significant difference between the Vestnesa and Storegga-margin cores in terms of thermal conductivity. Values are low (ca. 0.8–0.95 $W\,deg^{-1}\,m^{-1}$) in the top 3 m sampled in both pockmark areas. There is also little variability down the cores. This result is consistent with independent measurements of sound speed (low), wet bulk density (low), porosity (high), water content (high), and void ratio (high). The highest conductivity (0.9–0.95 $W\,deg^{-1}\,m^{-1}$) occurs at depths of 25–150 cm subbottom in core HM-11 (Fig. 9) located within or near a pockmark on the eastern Vestnesa Ridge. Because we cannot be certain whether this core was taken from the center or edge of a pockmark, the significance of these slightly enhanced values is unclear. The generally low thermal conductivities, a reflection of high water contents, are consistent with the acoustic "transparency" of the sediments (several tens of meters, Figs. 5 and 8).

Multiplying the thermal conductivity measured in these cores by the temperature gradients measured nearby (Table 1; Figs. 3B and 4B) yields the conductive heatflow. As noted above, the temperatures at the thermistors increased very linearly with subbottom depth, causing the error bars on the gradients to be modest. The gradients vary from 145 ± 9 and 140 ± 10 $mK\,m^{-1}$ on the western Vestnesa Ridge, to 116 ± 8 $mK\,m^{-1}$ on the eastern ridge, and down to 59.7 ± 1.9 and 56.2 ± 1.8 $mK\,m^{-1}$ on the Storegga margin. The resulting heatflow values are 123, 119, 104, 51, and 48 $mW\,m^{-2}$, respectively. These values are consistent with the regional pattern of heatflow (Figs. 2 and 6) and are qualitatively consistent with the location of the three surveyed areas: The western and eastern Vestnesa sites are located over oceanic crust ca. 7 and 10 million years old (Vogt et al. 1994), whereas the Storegga site is located over pre-Tertiary, probably thinned, continental crust. While we cannot rule out the existence of very local thermal anomalies, for example, in the centers of pockmarks, it can be concluded that no significant heatflow anomalies are associated with the pockmark areas. Furthermore, the attempt to measure heatflow both inside and outside a pockmark produced two pairs of values (119/123 and 48/51 $mW\,m^{-2}$) that are statistically identical. These results appear to rule out significant pore-water advection (except possibly very locally), because such advection would steepen thermal gradients above regional values (see Vogt and Sundvor 1996). For comparison, an extreme example of advection effects is provided by the Håkon Mosby mud volcano (Vogt et al. 1997).

Sediment physical properties

Sound speed, bulk density (from gamma-ray attenuation), porosity (calculated from bulk density), shear strength, water content, and grain size are shown plotted against subbottom depth for the Vestnesa Ridge cores in Fig. 10. The characteristic ranges are: wet bulk density, 1400–1600 $kg\,m^{-3}$; porosity, 65–75%; void ratio, 2.3–2.8; water content as percentage of dry weight, 60–120%; sound speed, 1480–1505 $m\,s^{-1}$; and shear strength, 3–12 kPa. Such values, consistent with the low thermal

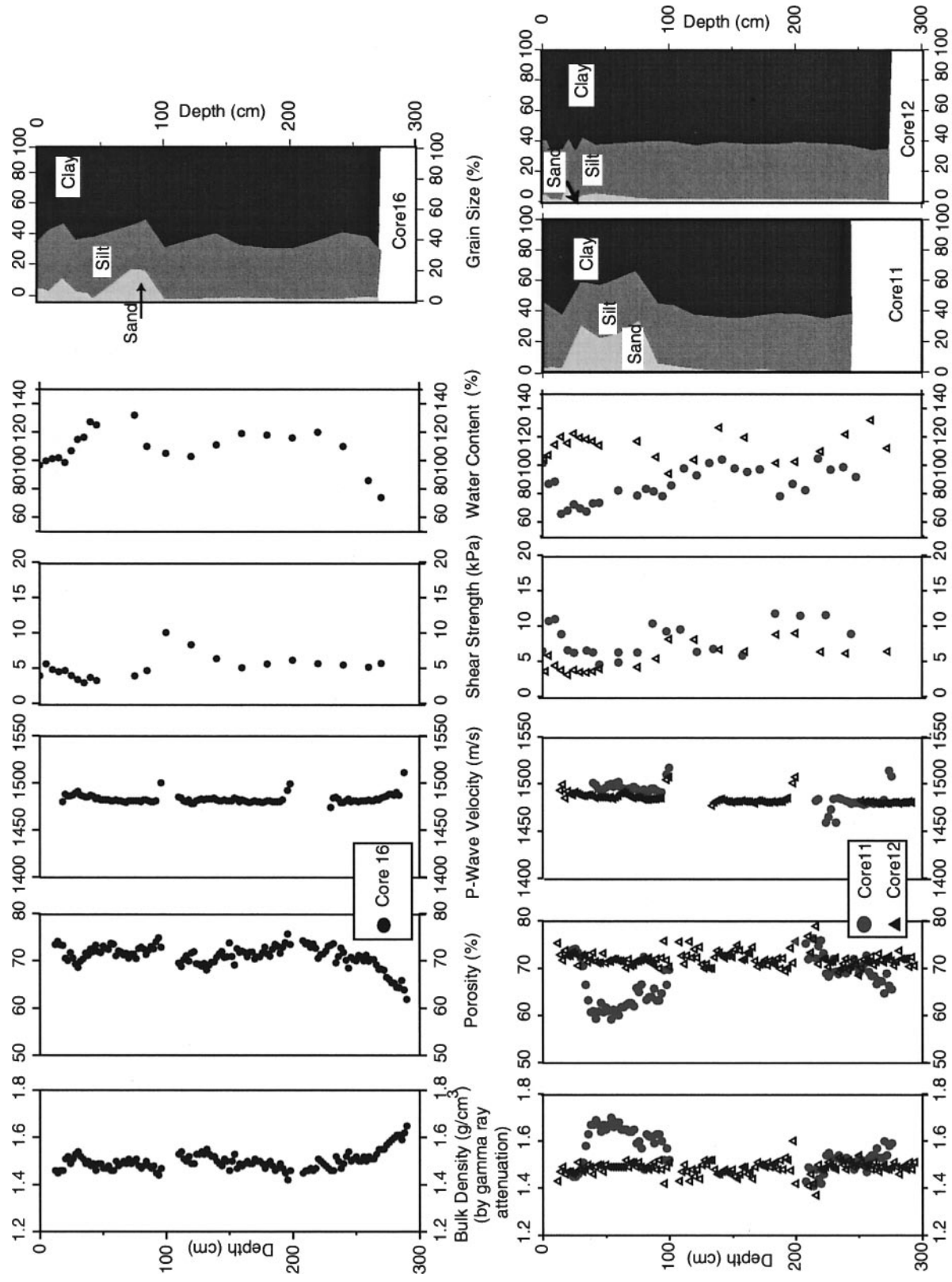

Fig. 10 Wet bulk density, porosity, and sound speed vs. subbottom depth, measured by logging of *Håkon Mosby* gravity cores (Sawyer et al. 1997), as well as water content, shear strength, and grain size from laboratory analysis of sediment sample. See Figs. 3B and 4B and Table 1 for locations

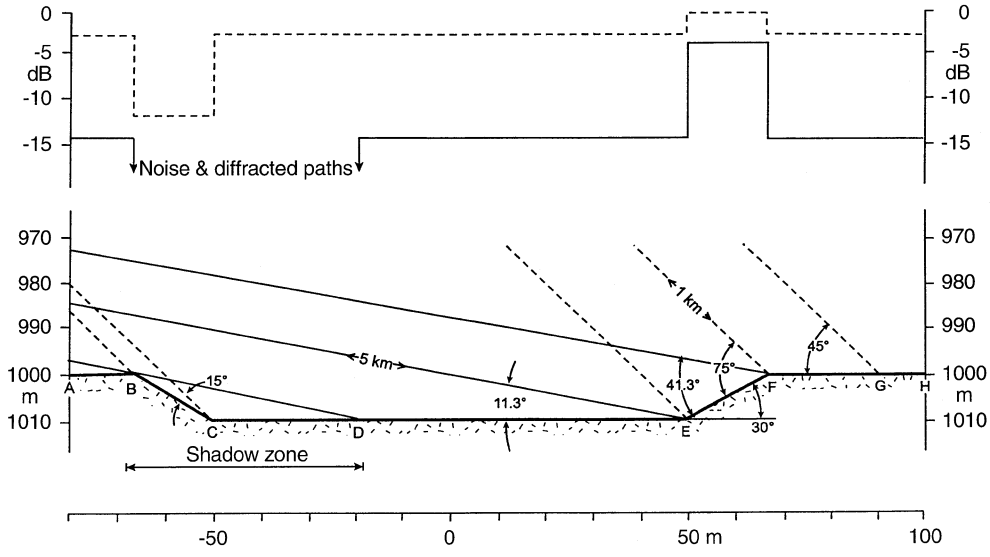

Fig. 11 Simple "ray" ensonification for a typical pockmark imaged from a surface-towed system at two ranges. Scattering strengths computed from simple "Lambert Law" scattering, neglecting effects of subbottom penetration

conductivities (Fig. 9), characterize the upper few meters of soft and watery sediment as typical for hemipelagic silty clay to clayey mud of postglacial (i.e., post-Weichselian) age, although micropaleontology has not been completed on the samples. Most of the cores 11, 12, and 16 comprise silty clays, with ca. 60% clay, a few percent sand, and almost 40% silt. However, the interval 25–75 cm in core HM-11, and to a lesser extent also in core 16, are sandier, with two samples of HM-11 containing more than 30% sand. It is unknown whether this sand increase represents increases in IRD (ice-rafted detritus) delivery or is a record of local pockmark activity. A downward increase in density and decrease in water content starting about 225–250 cm subbottom in core HM-16 (Fig. 10) could mark a downward increase in IRD abundance, but this should be accompanied by an increase in the sand fraction, which is not observed (Fig. 10). Thermal conductivity also increases at the bottom of this core (Fig. 9), as expected from the decreasing water content. However, core HM-12 appears not to have penetrated to this stratigraphic level. Hovland and Judd (1988) stated that pockmarks form preferentially in soft (vs. sandy) sediments, and we have substantiated and quantified their conclusion in terms of measured properties. (However, we expect that sediments below 3 m subbottom are rich in IRD and thus denser and less porous). Graphic evidence for the softness of pockmark-area sediments was also provided by the consistent full penetration (3 m) or overpenetration by our gravity cores, which did not occur at most other sites. Dark sediment with H_2S odor was not penetrated by the Vestnesa cores, nor were authigenic carbonate nodules captured, to judge from the physical properties.

The high empirical correlation between thermal conductivity and porosity assures us that sediments cored in the Storegga pockmark area have similar physical properties to those on the Vestnesa Ridge. Moreover, the observed H_2S odor and dark color, suggesting Fe monosulfides, in the core catcher of core PL-8 suggests that we successfully cored inside a pockmark (no. 9 in Figs. 7B and 8). We conclude this because methane ascent in the pockmark would raise the top of the sulfate reduction zone to shallower depths. Core PL-9 outside the pockmark did not penetrate H_2S-containing sediment. Nevertheless, the two cores are closely similar in their thermal conductivities and, by extrapolation, other physical properties. Significant amounts of sand left as a residual from pockmark formation (Hovland and Judd 1988) or authigenic carbonate nodules (present in some pockmarks; Hovland et al. 1987) were evidently not penetrated by the cores.

Discussion and summary

In 1995 and 1996 two areas in the Nordic Basin were revisited where 11- to 12-kHz side-scan sonar (SeaMARC II) had revealed a sea floor speckled with small spots (50–300 m across) with enhanced acoustic backscatter. Using bathymetry, shallow subbottom seismic profiling, sediment cores and heatflow stations, it could be confirmed that:

1. Most or all of the backscatter spots are pockmarks typically 2–10 m deep.

2. The sediments in the upper 3 m subbottom in and around the pockmarks are soft, porous (65–75%), and of low density (1400–1600 $kg\,m^{-3}$), low sound speed (1480–1505 $m\,s^{-1}$), and low thermal conductivity hemipelagic muds largely or entirely of Holocene age. The relatively uniform, low backscatter strength of the sea floor in which the pockmarks have formed is qualitatively consistent with the nearly constant subbottom sound speed and density measured in the cores, because such near-constancy implies weak volume scattering from

within the part of the sediment column, the top few meters, that influences 11- to 12-kHz backscatter imagery.

3. The Vestnesa, and possibly also the Storegga pockmarks, occur in a ca. 3-km-wide belt associated with a ridge crest, and formation may be inhibited on slopes greater than 20 : 1000.

4. The Vestnesa and Storegga pockmarks both occur in areas where BSRs (bottom simulating reflectors), indicating gas hydrates, have been identified in seismic data. The Storegga pockmarks are found 15–20 km north of the Storegga slide northern sidewall escarpment and may have been triggered by one or several of the slides described by Bugge et al. (1988). The location of the Storegga pockmarks along the older, buried sidewall escarpment described by Evans et al. (1996) is consistent with a preglacial initiation of fluid escape, although the Late Weichselian Storegga sliding may have stimulated fluid release along the older escarpment. Pockmarks have, to our knowledge, NOT been discovered within or above any of the slide scars mapped by SeaMARC II or other data, although they would be more difficult to recognize there. We concur with Evans et al. (1996), who suggest that slide and debris flows are not as likely to host hydrates and fluid-escape features as are thick sequences of stratified, porous hemipelagic and glacial marine sediments. The Vestnesa pockmarks occur above young (3–14 Ma) oceanic crust, and the Storegga pockmarks above subsided pre-Tertiary crust. The nature of the underlying deep crust is probably not relevant to their formation, however.

5. Both Vestnesa and Storegga pockmarks occur in areas of relatively high seismicity, so earthquakes could provide the most probable immediate trigger for episodic gas eruption and pockmark formation. The other triggering mechanisms suggested by Hovland and Judd (1988) are storms and tides. However, those forces would not create significant pressure changes at 900–1300 m water depths and are therefore not likely to play a role.

6. The Vestnesa and, probably, the Storegga pockmarks are not located above thermogenic methane "kitchens," so their origin must differ from that of most North Sea pockmarks (Hovland and Judd 1988).

7. Among the possible mechanisms for pockmark formation (Hovland and Judd 1988; Paull et al 1999), freshwater seeping and sea-floor freezing (Paull et al. 1999) probably cannot occur, given the fine, low-permeability sediments, the great distance to suitable terrestrial aquifers, and the stability of methane hydrates. Bottom-water temperatures average around -0.5°C in the pockmark areas, however (Vogt and Sundvor 1996), and if hydrate dissociation occurs, sufficiently fresh water might be produced to freeze in the pockmark bottoms.

8. Neither the Vestnesa nor the Storegga pockmarks exhibit heatflow anomalies relative to the regional averages. The relative heatflow differences between the two Vestnesa study areas and the Storegga area are readily explained by the differences in crustal age and origin. We can, however, not exclude very local anomalies in the pockmark centers, because the placement of our thermal probe was not that accurate and because we only sampled three, albeit prominent, pockmarks.

Conclusion

The reason why pockmarks show up exclusively as strong-backscatter spots (Figs. 3A, 4A, and 7A) remains uncertain. As shown in the ray-geometric diagram in Fig. 11, Lambert-law type scattering (Urick 1983) should produce, for a typical pockmark topography and uniform sediment properties, an acoustic shadow near the ship and enhanced backscatter immediately outboard of the shadow. In the SeaMARC II convention, there should be a white–black couplet, the white being closer to the ship. These topographic signals should be of significant amplitude, 2–7 dB (Fig. 11). The actual return would be smeared out, but the reasons why such smearing would invariably cause a strong backscatter spot are uncertain. One possibility is that the background backscatter is so weak that the pockmark acoustic shadow effect is limited by the noise floor, allowing the return from the far wall of the pockmark to dominate. Another possible effect is focusing, with the far side of the pockmark acting like a convex mirror to several successive pings, whose energy spread into the pockmark. Finally, there are a number of processes that would increase backscatter from the pockmark sea floor or from the shallow subbottom. Such effects, which are known to be associated with some pockmarks (Hovland and Judd 1988), include authigenic carbonate nodules or pavements, gas bubbles and pits/tubes, organisms such as clams, residual coarse sediment left behind from gas/fluid/mud eruptions, and small (unit) pockmarks. However, such processes are not plausibly at work in the "inactive" pockmarks, which simply exhibit down-bowed reflectors continuous under the features. Detailed pockmark inspections are needed to model the acoustic backscatter effects of pockmarks imaged by sidescan sonars and to identify the processes and levels and/or time scales of activity.

Acknowledgments This research was supported by the Office of Naval Research, Norsk Hydro, Statoil, and the Research Council of Norway. We thank shipboard scientists, officers, and crews of *F/S Håkon Mosby* and *NIS Professor Logachev* for supporting the 1995 and 1996 cruises. The Geology Department of the University of Bergen kindly lent box and gravity coring equipment. SeaMARC II data from the Storegga margin was collected in 1990 by H. Fleming, C. Nishimura, and others. Particular thanks to A. Nilsen for heatflow measurement assistance, and to W. B. Sawyer, L. Phelps, and W. R. Bryant for logging of sediment properties. P. Valent and especially M. Hovland provided careful reviews. Graphics and manuscript assistance were provided by I. Jewett and J. Brown.

References

Bugge T, Belderson RH, and Kenyon NH (1988) The Storegga slide. Philosophical Transactions of the Royal Society A 325: 357–358

Crane K, Sundvor E, Foucher J-P, Hobart M, Myhre AM, and LeDouaran S (1988) Thermal evolution of the western Svalbard margin. Marine Geophysical Researches 9 : 165–194

Crane K, Vogt PR, Sundvor E, Shor A, and Reed T IV (1995) SeaMARC II investigations off the northern Norwegian-Greenland Sea. In: Crane K and Solheim A (Eds.), Seafloor Atlas of the Northern Norwegian–Greenland Sea. Oslo: Norsk Polarinstitutt Meddelelser 137 : 32–140

Damuth JE (1978) Echo character of the Norwegian–Greenland Sea: relationship to Quaternary sedimentation. Marine Geology 28 : 1–36

Dowdeswell JA, Kenyon NH, Elverhøi A, Laberg JS, Hollender FJ, Mienert J, and Siegert MJ (1996) Large-scale sedimentation on the glacier-influenced polar North Atlantic margins: long-range sidescan sonar evidence. Geophysical Research Letters 23 : 3535–3538

Eiken O and Hinz K (1993) Contourites in the Fram Strait. Sedimentary Geology 82 : 15–32

Evans D, King EL, Kenyon NH, Brett C, and Wallis D (1996) Evidence for long-term instability in the Storegga Slide region of western Norway. Marine Geology 130 : 281–292

Hovland M and Judd AG (1988) Seabed Pockmarks and Seepages. London: Graham and Trotman, 293 pp

Hovland M, Talbot MR, Quale H, Olaussen S, and Aasberg L (1987) Methane-related carbonate cements in pockmarks of the North Sea. Journal of Sedimentary Petrology 57 : 881–892

Mienert J and Bryn P (1997) Gas hydrate drilling conducted on the European Margin. EOS 78 : 567, 571

Paull CK, Ussler W III, and Boroski WS (1999) Freshwater ice rafting: An additional mechanism for the formation of some high latitude submarine pockmarks. Geo-Marine Letters 19 : 164–168

Pfirman SL and Kassens H (1995) Seafloor echo character of the northern Norwegian-Greenland Sea. In: Crane K and Solheim A (Eds.), Seafloor Atlas of the Northern Norwegian-Greenland Sea. Oslo: Norsk Polarinstitutt Meddelelser 137 : 14–16

Sawyer WB, Bowles FA, Phelps L, Vogt PR, Crane K, Gardner J, Sundvor E, and Bryant WR (1997) Continuously logged sediment acoustical and physical properties data, *R/V Haakon Mosby* cores, Norwegian-Greenland Sea. Stennis Space Center, MS: Naval Research Laboratory, NRL/MR/7432-97-8041 : 165 pp

Shor A (1990) SeaMARC II seafloor mapping system: Seven years of Pacific Research. Parkville, Australia: Australian Institute of Mining and Metallurgy, Pacific Rim 90 Congress Proceedings: 12 pp

Sundvor E, Eldholm O, Gladczenko T, and Planke S (1999) Integrated Basin Studies, Special Issue. Journal of the Geological Society of London (in press)

Urick RJ (1983) Principles of Underwater Sound. New York: McGraw-Hill, 423 pp

Vogt PR and Sundvor E (1996) Heat flow highs on the Norwegian-Barents Svalbard continental slope: deep crustal fractures, dewatering, or "memory in the mud?" Geophysical Research Letters 23 : 3571–3574

Vogt PR, Crane K, Pfirman S, Sundvor D, Cherkis N, Fleming H, Nishimura C, and Shor A (1991) SeaMARC II sidescan sonar imagery and swath bathymetry in the Nordic Basin. EOS 72 : 486

Vogt PR, Crane K, Sundvor E, Max MD, and Pfirman SL (1994) Methane generated (?) pockmarks on young thickly sedimented oceanic crust in the Arctic: Vestnesa ridge, Fram strait. Geology 22 : 255–258

Vogt PR, Cherkashev G, Ginsburg G, Ivanov G, Milkov A, Crane K, Lein A, Sundvor E, Pimenov N, and Egorov A (1997) Haakon Mosby mud volcano provides unusual example of venting. EOS 78 : 549, 556–557

Wright JA and Louden KE (Eds.) (1989) Handbook of Seafloor Heatflow. Boca Raton, FL: CRC Press, 498 pp